JOURNAL OF MATERIALS SCIENCE 27 (1992) 6036–6040

Ionic conductivity in dehydrated zeolites

G. KELEMEN, G. SCHÖN
Institut für Anorganische Chemie der Universität Essen, Schützenbahn 70, W-4300 Essen 1, Germany

The ionic conductivity of pressed pellets of dehydrated synthetic offretite, cancrinite and zeolite A, with various alkali metal ions, was determined by low-frequency impedance spectroscopy. Experiments were carried out in the frequency range 10 Hz–10 MHz at temperatures from 100–600 °C. The conduction activation energies range between 55 kJ mol^{-1} (Na-zeolite A) and 108 kJ mol^{-1} (Li-cancrinite). The best conductivity value obtained was that of Na-zeolite A with $2.9 \times 10^{-3}\ \Omega^{-1}\ \mathrm{cm}^{-1}$ at 600 °C.

1. Introduction

Zeolites provide a broad field in the search for solid ionic conductors for applications, for example, in solid-state batteries or sensors. Because of their structure, zeolites offer good prerequisites to be fast ionic conductors due to their one-, two- or three-dimensional channel systems and their cation exchange ability. The conduction of zeolites is of an ionic nature and arises from the migration of cations in the crystalline zeolite framework [1]. In order to make assertions about the alkali metal conduction in zeolites, it is necessary to investigate them in the dehydrated state, because otherwise oxonium ions and/or hydroxyl ions could contribute to the conduction [2]. Among the numerous zeolites, only a few, e.g. zeolite X and Y [3–5] have been studied with respect to their ionic conductivity values. The electrical conductivity of anhydrous analcite and chabazite has been studied by Beattie [6]. Freeman and Stamires [7] reported the electrical conductivity of anhydrous zeolite A, X and Y. Recent investigations in the search for solid electrolytes have been carried out by Krogh-Andersen *et al.* [8] on alkali metal-zeolite X. Dielectric measurements of dehydrated zeolites have been performed [9, 10] so that statements about the mechanism of cation movement in zeolites could be drawn.

Here we present the second part of our investigations on the ionic conductivity of dehydrated zeolites. In a previous work [11], we reported the conductivity of dehydrated sodalite, analcime and offretite. To elucidate the possibilities of further improvement of ionic conductivities in zeolites, we have studied the influence of Si/Al ratio of the offretite framework on the ionic conductivity. Furthermore, conductivity values of alkali metal ions in cancrinite and zeolite A have been determined.

2. Experimental procedure

2.1. Synthesis and ion exchange

Offretite was synthesized according to the method given by Raeder [12]. The starting materials for the offretite synthesis were NaOH, KOH and aluminium strip (for analysis see Merck), SiO_2 sol (40 wt % Ludox HS 40) and $(CH_3)_4NOH$ (25 wt % in water). These chemicals were used in different concentrations so that offretite with distinct Si/Al ratios could be crystallized. This offretite contains in its synthesized form three monovalent cations which are TMA^+ (tetramethylammonium), K^+ and Na^+. The synthesis of azide-cancrinite followed a procedure described by Hund [13]. The chemicals used were NaOH and aluminium strip, sodium azide for synthesis and extra pure sodium silicate solution. Zeolite A was synthesized according to the method given by Barrer *et al.* [14] with NaOH, aluminium strip and sodium metasilicate.

The crystals were separated from the mother liquor by filtration and subsequently washed with distilled water. They were dried in air at 100 °C and stored in a desiccator over saturated $Ca(NO_3)_2$ solution before analysis. Silicon and aluminium were determined in the classical gravimetric manner. The alkali ion content of these products was determined by atom absorption spectroscopy (AAS) whereas the water content was thermogravimetrically determined. An organic microanalysis was performed to determine carbon, hydrogen and nitrogen in offretites containing organic cations and to determine nitrogen in cancrinite.

The desired ions were built in by the well-known methods of ion exchange from aqueous salt solutions with the above synthesized zeolites as starting materials [11]. The thermal decomposition of TMA^+ ions in offretite was carried out at 650 °C under a stream of oxygen before the ion-exchange process. Azide-cancrinite was heated to 600 °C for several hours to remove azide ions before ion exchange. After temperature treatment, only traces of nitrogen in the cancrinite could be detected by microanalysis.

X-ray diffraction patterns of all samples were determined to ascertain the structures of the zeolites. The thermal stability of the corresponding zeolites was examined up to 700 °C by differential thermal analysis (DTA).

Table I summarizes the synthesized and exchanged zeolites. The third column contains mol per cent ion content and should be read as follows: e.g. Li-zeolite A, 76% Li, means the residue up to 100% is 24% Na^+ as a result of incomplete ion exchange.

2.2. Preparation of compacts

Powder compressed discs with an average diameter of 13 mm and 0.3–0.5 mm thick were prepared at a pressure of 6×10^8 Pa at room temperature. The pellet density was 70%–75% of the single-crystal value. To increase the mechanical stability, zeolite compacts were heated in air at 400 °C for 24 h. A thin layer of platinum (0.1 µm) was vacuum sputtered on to both sides of the compact. After sputtering, the powder compacts were ground to a diameter of 5 mm.

2.3. Conductivity measurements

The measuring equipment with the high-temperature cell, and the data handling procedure are described elsewhere in detail [15, 16]. The applied technique of low-frequency impedance spectroscopy is undergoing a permanently developing process. The controlling processor HP 9825 that was earlier used in the impedance measurement system, is now replaced by an IBM compatible PC-AT. The latest development of the system is described in [17]; a more detailed publication will appear shortly.

The powder compact was inserted into the conductivity cell and heated at 400 °C for 1 h under an argon pressure of about 10 Pa. The impedance measurements were carried out from 10 Hz–10 MHz in 300 logarithmic equidistant frequency steps at each temperature using a Hewlett Packard LF impedance analyser HP 4192 A. All measurements were carried out in the temperature range 100–600 °C at intervals of 25 °C.

TABLE I Summary of the synthesized and ion-exchanged zeolites

Type of zeolite	Si/Al	Ion content (mol %)
Li-offretite	2.4:1	54 Li
Na-offretite	2.4:1	89 Na
K-offretite	2.4:1	57 K
Rb-offretite	2.4:1	35 Rb
Li-offretite	3:1	51 Li
Na-offretite	3:1	72 Na
K-offretite	3:1	98 K
Rb-offretite	3:1	63 Rb
Li-offretite	5:1	50 Li
Na-offretite	5:1	52 Na
K-offretite	5:1	100 K
Rb-offretite	5:1	78 Rb
Li-cancrinite	1:1	92 Li
Na-cancrinite	1:1	100 Na (originally synthesized)
K-cancrinite	1:1	42 K
Li-zeolite A	1.1:1	76 Li
Na-zeolite A	1.1:1	100 Na (originally synthesized)
K-zeolite A	1.1:1	94 K
Rb-zeolite A	1.1:1	59 Rb

3. Results and discussion

Ion conduction in zeolites is due to the migration of exchangeable cations along the channels and cavities of the zeolite framework according to an ion-hopping mechanism. In addition to dipol relaxations, it is the conduction of ions that causes responses in the frequency range between 10 Hz and 10 MHz. The ionic conductivity is determined by analysis of the a.c. measurements data in the complex impedance plane (Argand plot). The application of the complex plane method in analysing solid electrolyte measurements was introduced by Bauerle [18] and is now (to some extent further developed) largely accepted. The underlying model and the detailed method of measurement data evaluation was described previously [11].

Experimental data plotted in the complex impedance plane for K-zeolite A at different temperatures are shown in Fig. 1. These experimental data are typical for all of the other zeolites investigated. Characteristic features are the diffusion-related contribution at the interface platinum electrode/specimen which results in a spike inclined to the normal in the low-frequency range followed by a semi-circle in the direction of increasing frequencies. According to the model based upon [11], this semi-circle contains at least two relaxation phenomena which are not distinctly separated because the corresponding time constants lie close together. From the mutual intercept of the spike and the semi-circle on the z' axis at $z'' = 0$, the overall resistance of the system can be determined at each temperature. Taking into consideration the geometrical parameters of the pellet, the conductivity value may be obtained.

In plotting $\ln\sigma T$ as a function of the inverse of the absolute temperature, the activation energy may be determined according to the following equation (in a great deal of earlier work the factor $1/T$ was not considered and an empirical plot of $\ln\sigma$ versus $1/T$ was made. In a limited temperature range there is only

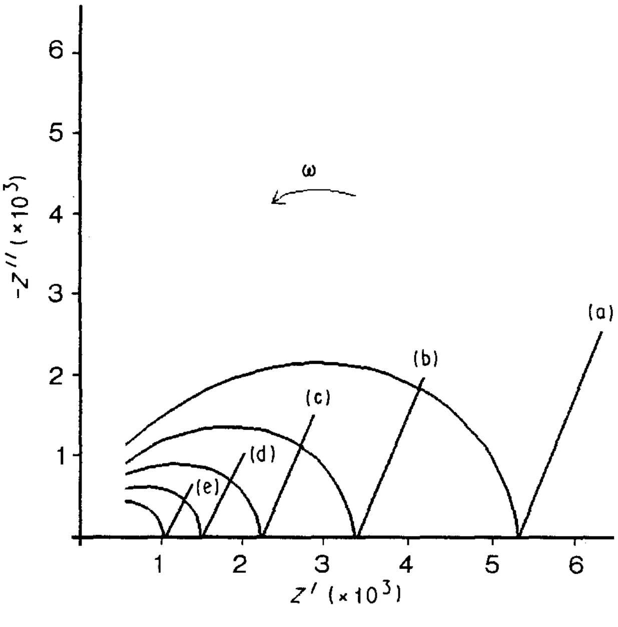

Figure 1 Experimental Argand plots for K-zeolite A at different temperatures. The arrow indicates increasing frequencies. (a) 300 °C, (b) 325 °C, (c) 350 °C, (d) 375 °C, (e) 400 °C.

a small change in the determined activation energy, but it should be kept in mind when comparing the results of different authors)

$$\sigma = 1/TA\exp(-\Delta H/RT) \qquad (1)$$

Over the examined temperature range, the Arrhenius plot gives a straight line as shown in Fig. 2 for offretite with Si/Al = 5. Variations in the activation energies determined for the same zeolite with several pellets extend to $\pm 3\,\text{kJ}\,\text{mol}^{-1}$ at maximum. These variations are mainly due to the pellet preparation process. The activation energies obtained from the Arrhenius plots are displayed against cation radius in Fig.3 . From the three zeolites investigated, Na^+ ions exhibited a minimum in activation energy.

Ionic conductivity in zeolites is determined by the electrostatic interaction between negatively charged framework and the mobile cations, as well as sterical effects caused by the ratio of size of cations and the narrowest points in the channel system. Furthermore, intercationic repulsions, especially for large ions and high ionic concentration, are to be considered likewise. In general, the coulombic interaction decreases with increasing cation radius, which is evident in Fig. 3 going from Li^+ ions to Na^+ ions. A decreasing electrostatic interaction causes a decreasing activation energy for ion conduction. In the case of K^+ and Rb^+, the increasing activation energy can be attributed to the sterical effects.

Tables II–IV give a survey of ionic conductivity values at different temperatures and activation energies of ionic conductivity. Table II includes the average result of two pellets of the same zeolite batch, whereas in Tables III and IV the results of one typical measurement are given. In comparison to ionic crystals, the deviation between the determined ionic conductivity values for different pellets of the same zeolite batch is relatively small. Winand and Depireux [19] reported a variation of a factor 6 for solid electrolytes. In the case of the investigated zeolites the variation gives a factor of 1.4 at maximum. For example, at 300 °C for two pellets of Na-zeolite A, the following ionic conductivity values were obtained: 6.1×10^{-5} and $8.3 \times 10^{-5}\,\Omega^{-1}\,\text{cm}^{-1}$.

The influence of different Si/Al ratios of the offretite framework on the ionic conductivity is shown in Table II. In the case of small ions (Li^+, Na^+), conductivity values decrease with increasing silicon content of the framework. Increasing silicon content signifies a decreasing number of negative charges per unit volume of the zeolite framework and a greater distance between negative charges. This great distance causes a longer path for cations in the ion-hopping process and results in a smaller value of ionic conductivity. In the case of larger ions (K^+, Rb^+) the best conductivity values are obtained from the sample with Si/Al ratio 3 (see Table II). For smaller Si/Al ratios, that is, in the case of a higher number of negative

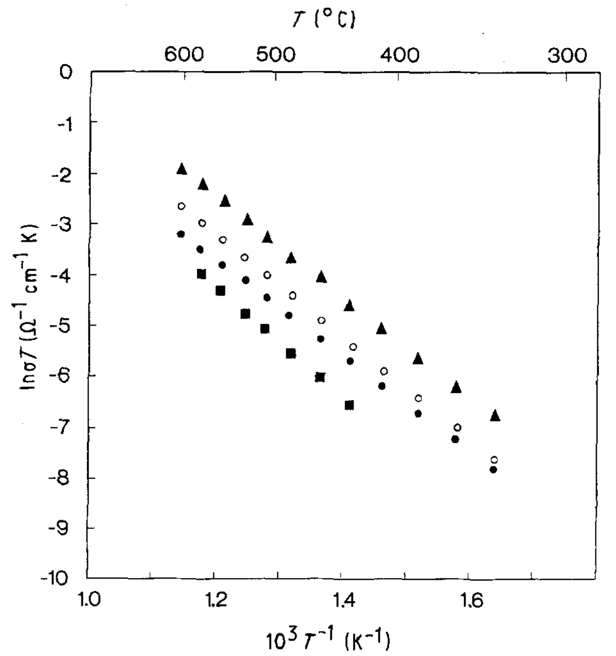

Figure 2 Arrhenius plot of offretite (Si/Al = 5), (○) Li, (▲) Na, (●) K, (■) Rb

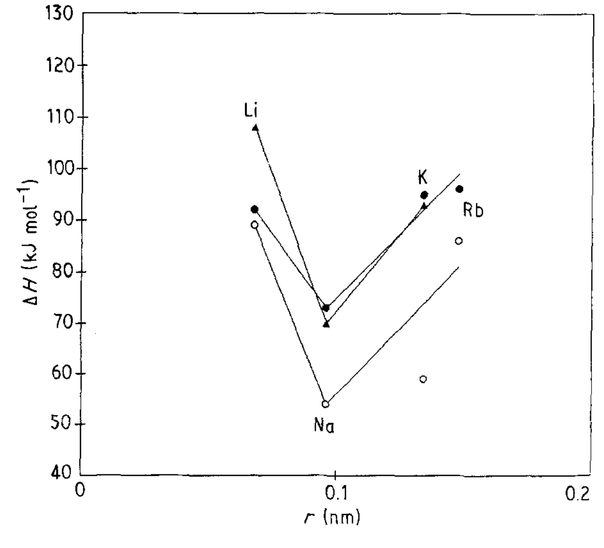

Figure 3 Dependence of the conduction activation energy on the cation radius. (●) Offretite (Si/Al = 2.4), (○) zeolite A, (▲) cancrinite.

TABLE II Ionic conductivities and activation energies of dehydrated offretite at different temperatures (mean value of the measurements of two pellets of the same zeolite batch)

Offretite (Si:Al)	$\sigma(\Omega^{-1}\,\text{cm}^{-1})$			ΔH (kJ mol^{-1})
	400 °C	500 °C	600 °C	
Li-offr. (2.4:1)	1.1×10^{-5}	8.2×10^{-5}	3.1×10^{-4}	92
Li-offr. (3:1)	1.2×10^{-5}	7.0×10^{-5}	2.5×10^{-4}	82
Li-offr. (5:1)	6.5×10^{-6}	3.6×10^{-5}	1.3×10^{-4}	78
Na-offr. (2.4:1)	7.9×10^{-5}	3.8×10^{-4}	1.2×10^{-3}	73
Na-offr. (3:1)	7.3×10^{-5}	2.4×10^{-4}	5.8×10^{-4}	61
Na-offr. (5:1)	9.0×10^{-6}	4.5×10^{-5}	1.4×10^{-4}	75
K-offr. (2.4:1)	3.2×10^{-6}	2.5×10^{-5}	1.2×10^{-4}	95
K-offr. (3:1)	1.2×10^{-5}	6.4×10^{-5}	2.0×10^{-4}	74
K-offr. (5:1)	3.2×10^{-6}	1.5×10^{-5}	4.8×10^{-5}	73
Rb-offr. (2.4:1)	2.2×10^{-6}	1.9×10^{-5}	9.0×10^{-5}	96
Rb-offr. (3:1)	6.3×10^{-6}	4.1×10^{-5}	1.7×10^{-4}	84
Rb-offr. (5:1)	1.2×10^{-6}	6.9×10^{-6}	2.6×10^{-5}	82

TABLE III Ionic conductivities and activation energies of dehydrated zeolite A at different temperatures (one typical measurement of each zeolite)

Zeolite A	$\sigma(\Omega^{-1}\,cm^{-1})$					ΔH (kJ mol^{-1})
	200 °C	300 °C	400 °C	500 °C	600 °C	
Li-zeol.	–	8.8×10^{-7}	1.1×10^{-5}	9.0×10^{-5}	4.6×10^{-4}	90
Na-zeol.	9.0×10^{-6}	8.3×10^{-5}	3.8×10^{-4}	1.2×10^{-3}	2.9×10^{-3}	55
K-zeol.	3.1×10^{-6}	3.5×10^{-5}	1.8×10^{-4}	6.0×10^{-4}	1.4×10^{-3}	59
Rb-zeol.	–	8.3×10^{-8}	8.3×10^{-7}	5.6×10^{-6}	2.6×10^{-5}	86

TABLE IV Ionic conductivities and activation energies of dehydrated cancrinite at different temperatures (one typical measurement of each zeolite)

Cancrinite	$\sigma(\Omega^{-1}\,cm^{-1})$				ΔH (kJ mol^{-1})
	300 °C	400 °C	500 °C	600 °C	
Li-can.	–	6.0×10^{-7}	5.6×10^{-6}	3.9×10^{-5}	108
Na-can.	1.2×10^{-5}	8.1×10^{-5}	3.7×10^{-4}	1.5×10^{-3}	70
K-can.	–	2.9×10^{-6}	2.5×10^{-5}	1.0×10^{-4}	94

framework charges and a higher concentration of charge-compensating cations, the ionic conductivity decreases, contrary to the case for smaller ions (Li^+, Na^+). In addition, repulsive interactions between the bigger cations which counteract ion conduction have to be considered. All together, it can be stated that ionic conductivity in zeolites may be influenced by variation of the framework Si/Al ratio, whereby for offretite the improvement in conductivity values is in the range of about one order of magnitude. Conductivity values for the small cations (Li^+, Na^+) are better in offretite with a small Si/Al ratio (about 2.4) whereas for larger ions (K^+, Rb^+) a middle Si/Al ratio of about 3 (see Table II) is preferred.

Assuming similar grain-boundary effects of the same magnitude in all investigated zeolites because of uniform sample preparation and thermal pretreatment, the dependency between structure and ionic conductivity may be discussed. To possess high ionic conductivity, the crystal structure must have clearly defined open diffusion paths with an optimum channel size. Thus, if the channels are too large in diameter, ions end to stick at sites in the cavities and channel walls. On the other hand, channels and bottlenecks in the channel system must be large enough because of sterical reasons.

When the three investigated zeolites are compared, the best ionic conductivity is obtained in zeolite A for Li^+, Na^+ and K^+. Na-zeolite A gives a conductivity value of $2.9\times10^{-3}\,\Omega^{-1}\,cm^{-1}$ at 600 °C, which is, to our knowledge, the best value at this temperature ever determined in zeolites.

In cancrinite, a strong dependency of ionic conductivity on temperature is evident. Only at relatively high temperatures (above 400 °C) are ionic conductivity values of Li^+ and K^+ high enough for reliable measurements. In addition to wide channels parallel to the c-axis (free diameter ~ 0.62 nm) the cancrinite structure possesses smaller diffusion paths (six rings of about 0.23 nm free diameter), which plays a role, probably only at higher temperatures. Furthermore, stacking faults may block the wide channels by six rings [20]. These are the reasons for the stronger increase of ion conduction only at higher temperatures.

The conduction of Na^+ and K^+ ions in cancrinite is almost identical to that in offretite (2.4) over the investigated temperature range. This may be attributed to similar structural features of the two zeolites; offretite also has relatively wide channels parallel to the c-axis. The ionic conductivity of Li^+ in cancrinite is unexpectedly small and is about one order of magnitude smaller in comparison to offretite (2.4) and zeolite A. This may be explained as a result of framework destruction during ion exchange, for which X-ray diffraction patterns give some indications.

Na^+ ions give the best conductivity values in the investigated structures. In Fig. 4, Na-zeolite A is arranged in the field of solid electrolytes. An Arrhenius plot of log σ against reciprocal temperature is shown.

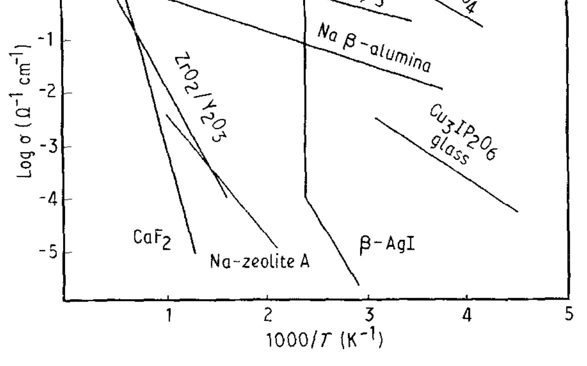

Figure 4 Conductivity data of several solid electrolytes. (For comparison a strong liquid electrolyte, concentrated H_2SO_4, is shown.)

The ionic conductivity is several orders of magnitude lower in comparison with the well known Na^+ ion conductor β-alumina.

4. Conclusion

The ionic conductivity values of alkali metal ions in dehydrated offretite, cancrinite and zeolite A have been determined. Na^+ ions show the best conduction in the investigated zeolite structures. The highest conductivity value is reached in Na-zeolite A which is $2.9 \times 10^{-3}\ \Omega^{-1}\,cm^{-1}$ at 600 °C. For the smaller Li^+ ions and the larger K^+ and Rb^+ ions, conductivity values are lower because of electrostatic and steric reasons, respectively. The influence of framework Si/Al ratio in offretite on ion conduction is shown. Ionic conductivity follows an Arrhenius behaviour and conduction activation energies range between $55\ kJ\,mol^{-1}$ (Na-zeolite A) and $108\ kJ\,mol^{-1}$ (Li-cancrinite).

In the field of solid electrolytes (Fig. 4), zeolites are rather in the middle range as far as their ionic conductivities are concerned. To approach the practical desired value of about $10^{-1}\ \Omega^{-1}\,cm^{-1}$ at room temperature seems to be rather far away. This is a structural question of all zeolites. Large channels and cavities at the intersection points of the diffusion paths cause relatively high potential barriers and the ions partly become immobilized at sites displaced from the centres of the channels and cavities.

Acknowledgement

This work was supported by the Federal Office of Research and Technology (BMFT) of the Federal Republic of Germany under contract no. 0328565 B. The content of this article is the authors own responsibility.

References

1. D. C. FREEMAN Jr and D. N. STAMIRES, *J. Chem. Phys.* **35** (1961) 799.
2. E. KROGH ANDERSEN, I. G. KROGH ANDERSEN, E. SKOU and S. YDE ANDERSEN, in "Solid State Protonic Conductors", edited by J. B. Goodenough, J. Jensen and A. Potier, Vol. 3 (Odense University Press, Odense, 1985) p. 100.
3. R. A. SCHOONHEYDT, in "Proceedings of the Fifth International Conference on Zeolites", Naples, Italy, June 1980, edited by L. V. C. Rees (Heyden, London, 1980) p. 242.
4. R. A. SCHOONHEYDT and J. B. UYTTERHOEVEN, in "Molecular Sieve Zeolites I" (American Chemical Society, Washington, DC, 1971) p. 456.
5. R. A. SCHOONHEYDT and W. DE WILDE, *J. Chem. Soc. Faraday Trans. I* **70** (1974) 2132.
6. I. R. BEATTIE, *Trans. Faraday Soc.* **50** (1954) 581.
7. D. C. FREEMAN Jr and D. N. STAMIRES, *J. Chem. Phys.* **35** (1961) 799.
8. E. KROGH ANDERSEN, I. G. KROGH ANDERSEN, J. METCALF-JOHANSEN, K. E. SIMONSEN and E. SKOU, *Solid State Ionics* **28–30** (1988) 249.
9. T. OHGUSHI, *Bull. Chem. Soc. Jpn* **61** (1988) 1109.
10. T. OHGUSHI and S. SATO, *J. Solid State Chem.* **87** (1990) 95.
11. G. KELEMEN, W. LORTZ and G. SCHÖN, *J. Mater. Sci.* **24** (1989) 333.
12. J. H. RAEDER, *Zeolites* **4** (1984) 311.
13. F. HUND, *Z. Anorg. Allg. Chem.* **509** (1984) 153.
14. R. M. BARRER, J. W. BAYNHAM, F. W. BULTITUDE and W. M. MEIER, *J. Chem. Soc.* **1** (1959) 195.
15. W. LORTZ, PhD thesis, University of Essen (1987).
16. W. LORTZ, W. OSSWALD, G. KELEMEN and G. SCHÖN, *J. Phys. E Sci. Instrum.* **22** (1989) 293.
17. E. THOMAE, PhD thesis, University of Essen (1990).
18. J. E. BAUERLE, *J. Phys. Chem. Solids* **30** (1969) 2657.
19. J.-M. WINAND and J. DEPIREUX, *Europhys. Lett.* **8** (1989) 447.
20. R. M. BARRER and D. E. W. VAUGHAN, *J. Phys. Chem. Solids* **32** (1971) 731.

Received 26 June 1991
Accepted 7 February 1992